Microscale droplet absorption into paper for inkjet printing

Anna Lundberg, Jonas Örtegren, Elisabeth Alfthan, and **Göran Ström**

KEYWORDS: Paper properties, High-speed inkjet printing, Capillary absorption, Lucas-Washburn equation, Dyes

SUMMARY: Digital printing using high-speed inkjet technology puts heavy demands on paper's ability to rapidly absorb the liquid into the paper. This is important for both the runability during the printing process and for the print quality. In this article, the dynamics of inkjet droplet absorption and penetration is discussed. The Lucas-Washburn equation has been applied to experimental results from inkjet printing on paper. The ink absorption on different paper grades is discussed in terms of the physical properties of the surface such as surface energy, surface roughness and porosity.

The results of this study indicate that ASA used as internal sizing reduces the absorption speed of water based dye inkjet ink and that evaporation affects the result. The Lucas-Washburn equation can be used to some extent for describing micro-scale droplet absorption into paper, depending on the properties of the paper.

ADDRESSES OF THE AUTHORS: Anna Lundberg (anna.lundberg@miun.se) and **Jonas Örtegren,** (jonas.ortegren@miun.se): Digital Printing Center / Mid-Sweden University, SE-891 18 Örnsköldsvik, Sweden**, Elisabeth Alfthan,** Kommendörsgatan 44, SE-114 58 Stockholm / Sweden, **Göran Ström** (goran.strom@innventia.com): Innventia / SE-114 86 Stockholm, Sweden
Corresponding author: Jonas Örtegren

Until today, the main advantages with digital printing have been the possibilities of short runs and variable data printing. One of the limitations for using inkjet printing for long production runs has been the low printing speed. The development of the inkjet technology has however led to a break through concerning the paper feeding speeds at which inkjet printing can be operated, resulting in a continuously increasing amount of high-speed inkjet machines for industrial print production. Inkjet printing at a high paper feeding speed puts severe constraints on the combination of inkjet technology, paper and ink to improve the runability and to maintain a high print quality. Thereby an increased need has come for understanding the dynamic processes that take place during printing as inkjet droplets spread and absorb into paper media. In inkjet printing, the print quality is directly associated to the imbibition process (Holman et al. 2002). The spreading of the droplet affects the resolution and the colour gamut volume. Droplet spreading is affected by the surface energy and the surface roughness of the substrate. The dynamic behavior of the spreading of droplets of surfactant solutions on non-porous substrates with varying hydrophobicity has been studied by von Bahr et al. (2003). To avoid bleeding and droplet coalescence fast penetration of the liquid is desirable, but the colorant of the ink should not penetrate deep into the substrate in order to reproduce a large colour gamut volume.

Paper as material is a complex porous structure and may be described as a network of randomly distributed capillaries. Several studies of droplet dynamics on porous substrate have been made during the last few years (Clarke et al. 2002, Starov et al. 2002, Blake et al. 1997, Davis, Hocking 1999, 2000, Alleborn, Raszillier, 2004, 2007, Modaressi, Garnier, 2002, Heilmann, Lindqvist, 2000,a, Heilmann, Lindqvist, 2000,b, Denesuk et al. 1994, Daniel, Berg 2006, Lavi et al. 2008). One theory for describing the dynamics of liquid flow into a capillary was derived by Lucas (1918) and Washburn (1921). The Lucas-Washburn equation describes the dynamic motion of an infinite amount of fluid into an empty capillary driven by the Laplace pressure incorporated into Poiseuille's equation. This equation has been tested and questioned over the years (Fisher, Lark 1979, Danino, Marmur, 1994, Lee et al. 2008). Two of the parameters that Lucas-Washburn does not take into account are the effect of inertia (Bosanquet 1923) and dynamic contact angle (Joos et al. 1990, Siebold et al. 2000, Martic et al. 2002).

In 1923, Bosanquet (1923) derived an equation adding inertial forces to the Lucas-Washburn equation. It has later been found that the effect of inertia is very small for small pores (<1 um) (Schoelkopf, Gane et al. 2000, Ridgway et al. 2002, Schoelkopf, Ridgway et al. 2000). The Davis-Hocking model (1999, 2000) states that the available surface for sorption diminishes during absorption. Application of the Lucas-Washburn equation and Davis-Hocking theories on inkjet printing has been made. Desie and Van Roost (2006) describe differences during the imbibition process for dye based and pigmented inks compared to Lucas-Washburn and Davis-Hocking. For hydrophobic paper, it has been found that the penetration mechanisms are primarily affected by

diffusion and the driving potential for liquid transport into porous material is the sum of the external pressure, and the capillary and diffusion potentials (Salminen 1988).

This study focuses on absorption of dye based ink into different fine paper grades. Absorption of picolitre droplets on paper samples with known composition has been studied and compared to the Lucas-Washburn theory. The droplets were ejected from an inkjet print head. The kinetic energy of the inkjet ink droplet was not considered in the physical description.

Materials and Methods

Paper: Seven paper samples were investigated. Three of the papers (Papers 1, 2 and 3) were pilot papers manufactured at low production speed (approximately 2 m/min) in a small paper machine at MoRe Research (Lundberg et al. 2009). Four of the papers were commercial papers: two coated inkjet papers (Papers 4 and 5), one uncoated high speed inkjet paper (Paper 6) and one uncoated office paper (Paper 7). The papers are listed in *Table 1*. The pilot papers were not surface treated, uncoated and not calendared. All pilot papers contained 75% hardwood (HW) and 25% softwood (SW). Paper 1 was made as the reference paper and its composition is similar to a regular office paper, however without internal sizing agent. The hardwood in Paper 1 and Paper 2 was mainly birch, while it was eucalyptus in Paper 3. All papers contained mainly pine as softwood. In difference to Paper 1, Paper 2 was internally sized with alkyl succinic anhydride (ASA). The pilot papers all contained the same starch (cationic potatoe starch), filler (precipitated calcium carbonate) and retention aid (cationic polyacrylamide and anionic sodium bentonite), and the same amount thereof.

Paper surface characteristics: The porosity of the papers was characterized by Hg-porosimetry using Autopore IV 9500 from Micrometrics according to ISO/WD 1590-1. The maximum applied pressure of mercury (surface tension: 485 mN/m) was 2000 bar corresponding to pores about 0.01 µm and a contact angle of 140°. Data for pore sizes up to 10 µm was analysed. Surface roughness was measured with the Bendtsen method. Static contact angle measurements were made with a Fibro DAT1100 on 4 µl of water and 3 µl diiodmethane after 0.1 seconds of contact between the droplet and the substrate. The surface energy was derived from Young's equation together with the work of adhesion based on the geometric mean model and calculated according to TAPPI T 558 om-97 (TAPPI). Due to the uncertainties associated with the rapid absorption of fluid into the porous substrate, the term apparent surface energy is used below. Separate static contact angle measurements with ink from the printing system were also made. Images of the distribution of single inkjet droplets deposited onto the paper samples were taken after printing by light microscopy with 430 x magnification (cross section images) and with 210 x magnification (top view; shape and size of dot).

Table 1. Papers investigated in this study.

No	Comment	Paper grade	Production	Gram-mage [g/m²]	Thick-ness [µm]	Sheet density [kg/m³]
1	Reference	Office	Pilot-made	93.6	135	696
2	Internally sized	Office	Pilot-made	92.9	129	719
3	Eucalyptus & pine pulp	Office	Pilot-made	92.2	142	648
4	Inkjet Coated	Coated Inkjet	Commercial	98.6	117	843
5	Inkjet Coated	Coated Inkjet	Commercial	107	137	785
6	High Speed	Uncoated Inkjet	Commercial	90.4	120	686
7	Copy	Office	Commercial	80.6	110	753

Printing system: A KODAK Versamark DS 5240 printhead was used to eject 40 pl droplets onto the paper surface (paper property measurements and inkjet printing on each paper were made on the same side of the paper). The KODAK Versamark printhead is a single pass continuous printing system which allows printing speed up to 5 m/s. The ink used in the printhead was commercially available water based dye ink suitable for the KODAK Versamark printhead (FD 1007 black ink). The ink viscosity was determined to 1.32 mPa·s by using an Ubbelohde viscosimeter. The surface tension of the ink was determined to 39.5 mN/m by the pendant drop shape method. The density of the ink was 1.006 g/cm^3.

Camera system: A high-speed camera, Redlake Motion Pro 10000 was used to capture images of 1280 x 256 pixels at a frame rate of 2000 fps and 20 times magnification and a resolution test target of Melles Griot was used to measure the size of one pixel in the image. The used pattern on the test target consisted of 14.3 lines/mm and the measured pixel edge length was 0.7 µm. Schott DCR III lightning was used as light source. To be able to get a sharp image, the camera had to be tilted approximately 3 degrees.

Image analysis: The High Speed Camera was used for capturing images of the droplets from the side. A MatLab program was used to separate the pixels of the grayscale picture that belonged to the droplet from those that did not. The threshold value for separating the pixels was defined by capturing an

image without the droplet and the minimum and maximum of its histogram represent the thresholds for the separation.

The height and diameter of the droplet could be measured from the captured images. Based on the assumption that the droplet has the form of a spherical cap *(Fig 1)* the volume of the ink-droplet above the paper surface could be calculated by using *Eq 1*.

$$V = \frac{\pi}{6} \cdot H \cdot \ (3a^2 + H^2) \qquad [1]$$

where *H* and *a* are the height and the radius of the cap, respectively.

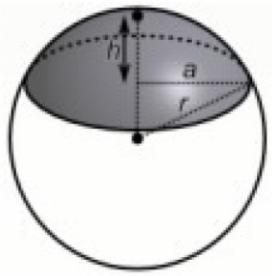

Fig 1. Spherical cap where r is the radius of the sphere, h the height of the cap, and a the radius of the cap. The spherical cap is a model of the shape of the inkjet ink droplet above the paper surface as it absorbs into the paper.

Because of the tilting of the camera, the volume had to be corrected according to *Eq 2*.

$$H = h(1 - \sin\left(\theta_{camera}\right)) \qquad [2]$$

where h represents the uncorrected height, θ_{camera} the angle of tilting the camera and h represents the measured height.

Absorption: The absorbed volume, i.e. the volume below the paper surface was calculated from the volume loss above the surface according to *Eq 3*.

$$V_{below} = V_{initial} - V_{above} - V_{evap} \qquad [3]$$

Where V_{below} represents the volume below the surface, i.e. the absorbed volume, V_{above} represents the volume above the surface, V_{evap} is the evaporated volume.

Penetration depth: Based on the assumption that the volume below the surface has the form of a paraboloid, the experimental penetration depth $d_{exp}(t)$ could be calculated from *Eq 4*.

$$V(t)_{below} = \frac{\pi \cdot R(t)^2}{2} \cdot d_{exp}(t) \qquad [4]$$

where *R* represents the radius of the droplet. If instead the volume below the surface has a cylindrical form, the penetration depth can be calculated from *Eq 5*.

$$V(t)_{below} = \pi \cdot R(t)^2 \cdot d_{exp}(t) \qquad [5]$$

A light microscope was used to take cross section images in order to determine the ink distribution of the samples.

Lucas-Washburn equation: The Lucas-Washburn equation was derived for penetration of liquids into cylindrical capillaries in the absence of a gravitational field (Lucas 1918, Washburn 1921). Washburn applies Poiseuille's law for fluid motion in a circular tube according to *Eq 6*.

$$dV = \frac{\pi \cdot \sum P}{8\eta \cdot d(t)} (r^4 + 4\epsilon^3) dt \qquad [6]$$

where dV describes the differential volume of the liquid that flows during the differential time, dt, η is the viscosity of the fluid, ϵ is the coefficient of slip. ΣP is the total effective pressure acting to force the liquid into the capillary which is the sum of the participating pressures, such as the atmospheric pressure, the hydrostatic pressure and the equivalent pressure due to capillary force, r, represents the radius of the capillary.

Under the assumption that the coefficient of slip is zero for wetting materials and for capillaries so small, that the external pressure can be neglected, the penetration depth according to Lucas-Washburn, $d_{LW}(t)$, can be expressed as proportional to the square root of time (Washburn 1921).

$$d_{LW}(t) = k_{LW} \sqrt{t} = \sqrt{\frac{\gamma \cdot r \cdot cos\theta}{2\eta}} \sqrt{t} \qquad [7]$$

where γ represents the surface tension of the liquid and θ represents the contact angle. The applicability of the Lucas-Washburn equation for describing droplet absorption according to the conditions described here was evaluated by slightly modifying *Eq 7*:

$$V_{below}(t) = \frac{N}{A} \pi R(t)^2 \cdot \pi \cdot r^2 \cdot d_{LW}(t) \qquad [8]$$

where *N/A* is the number of capillaries per unit area.

Results

Below, the result from absorption measurements of single inkjet droplets in paper samples is presented. The absorption process is described by utilizing the Lucas-Washburn equation after introducing corrections for evaporation, and by taking the ratio between void and paper media into account and adjusting for a large number of capillaries. *Fig 2*

illustrates the differential pore distribution of the papers. Based on Hg porosimetry data and knowledge about the different paper grades, one representative pore size per paper grade was selected. Papers 1, 3 and 7 exhibit a narrow peak around 0.35 µm whereas Paper 6 exhibits a wider peak between 0.1 and 2.2 µm. In the case of the coated Paper 5, a peak at a pore size of about 1.7 µm was interpreted as originating from the base paper. The Hg porosimetry measurements on the coated papers (Paper 4 and 5) indicate that the pores in the coating layer are smaller than 0.03 µm (all data not shown). Small peaks at about 5 µm appearing mainly in Paper 1 and Paper 3, but also in Paper 2, were interpreted as originating from surface pores.

The results from measurements of surface roughness, pore size, apparent surface energy and apparent static contact angle of the ink are presented in *Table 2*. The differences in the surfaces between the coated papers (Paper 4 and 5) and the uncoated papers, is reflected in the lower porosity, the smaller pore size, and the lower surface roughness of Papers 4 and 5. The surface roughness of the uncoated papers showed small variations. Paper 6 exhibited the highest surface roughness. The apparent surface energy data should be treated with some caution due to the rapid absorption of fluid into the porous substrate. The low apparent surface energy of Paper 2 can be explained by the internal sizing in this paper. The low apparent surface energy of the commercial office Paper 7 is mainly due to the amount of internal sizing, but also to differences in surface treatment.

Table 2. Paper properties.

No	Rough-ness [ml/min]	Void Volume $\left[\frac{cm^3}{m^2}\right]$	Pore size peak $[\mu m]$	Surf. Sizing	Int. Sizing	App. Surf energy *[mN/m]*	App. static contact angle (ink)
1	278	38	0.35	No	No	75.9	17.6
2	242	43	0.35	No	Yes	35.0	85.5
3	238	38	0.35	No	No	77.0	17.6
4	68	15	<0.03	No info	No info	73.1	18.5
5	39	10	<0.03	No info	No info	55.0	41.9
6	322	38	2.1	Yes	No	57.0	46.5
7	272	31	0.35	Yes	Yes	32.4	70.9

According to data retrieved with the methods used in this study, the differences in properties between Paper 1 and Paper 3 were smaller than for the other samples, and some graphs from measurements on Paper 3 are therefore left out below. Representative cross section images of single inkjet droplets deposited onto the paper samples are depicted in *Fig 3*.

It was found that the shape of the droplet below the surface differed for the different samples. It is here assumed that, during absorption, the shape of the droplet below the surface can be represented by the experimentally determined ink distribution in the papers after absorption. In the pilot papers (Papers 1 and 2 are shown in *Fig 3*) the ink distribution appeared more or less like a paraboloid, whereas for the coated papers (Paper 4 and 5) the ink distribution was cylindrical. The colorant of the ink does not seem to penetrate into the base paper in the case of the two coated papers. For the commercial office paper (Paper 7), almost no ink can be visualized below the surface in the cross section image, indicating that the dyes stay mainly on the surface.

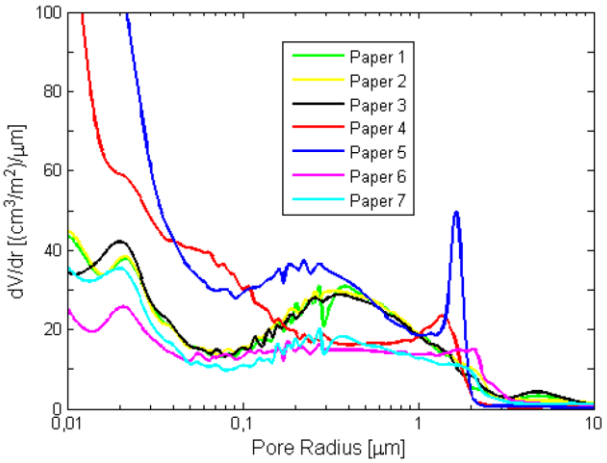

Fig 2. Differential pore size distributions obtained for Papers 1-7.

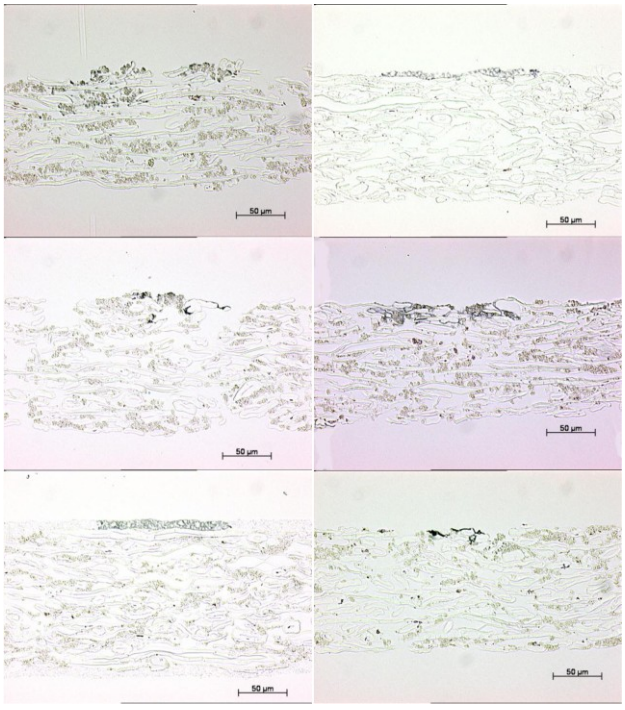

Fig 3. Cross section images of ink distribution. Top to bottom, left: Papers 1, 2, and 4, right: Papers 5, 6 and 7.

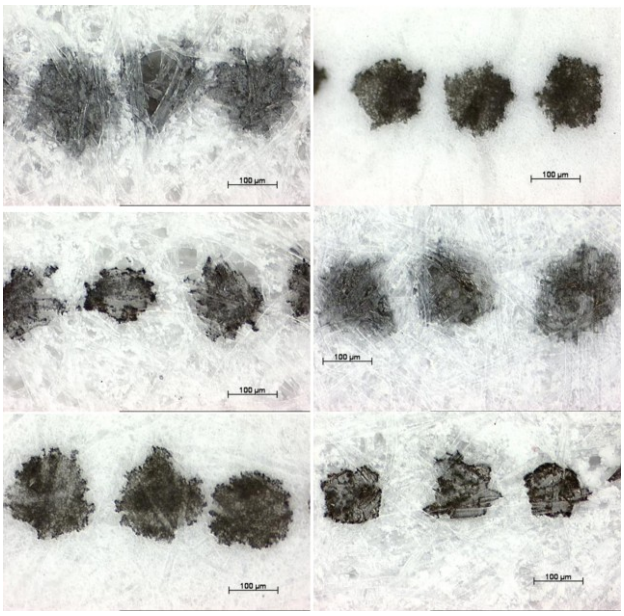

Fig 4. Images of inkjet printed dots. Top to bottom, left: Papers 1, 2, and 4, right: Papers 5, 6 and 7.

Light microscopy images of inkjet printed dots on the various papers are shown in *Fig 4*.

Inkjet printing on the papers with a high apparent surface energy (Paper 1, 3 and 4) resulted in large dots, whereas the opposite holds for the low apparent surface energy papers (Paper 2 and 7). Paper 5 exhibited relatively small dots with good roundness, which may be due to the low surface roughness of this paper. Paper 4 has also a low surface roughness, but this is obviously less important than the difference in surface energy.

Inkjet printing on the papers with a high apparent surface energy (Paper 1, 3 and 4) resulted in large dots, whereas the opposite holds for the low apparent surface energy papers (Paper 2 and 7). Paper 5 exhibited relatively small dots with good roundness, which may be due to the low surface roughness of this paper. Paper 4 has also a low surface roughness, but this is obviously less important than the difference in surface energy.

Five side-view film sequences per paper of droplet absorption during inkjet printing were recorded. An example of a film sequence of a droplet on a paper surface is depicted in *Fig 5*. The repeatability of the measurements was good and showed reliable trends regarding absorption as function of time, indicating both that the experimental set-up was stable and that local variations in paper properties did not largely affect the absorption behavior when measured accordingly.

The height and radius of the droplet were analyzed as a function of time and the volume was calculated according to eq. 1. The mean value of the volume above the paper surface was calculated for each sample, and is illustrated in *Figs 6* and *7*. It is shown in *Fig 6*, that the ink absorption was much slower for the internally sized pilot paper (Paper 2) than for the other (unsized) pilot papers (Paper 1 and 3). There is only a small difference in absorption rate between Paper 1 and Paper 3 (inset, *Fig 6*).

The mean value of the ink volume above the paper surface for the commercial paper grades has been plotted as a function of time in *Fig 7* (Paper 4, 5, 6 and 7). The absorption rate for the internally sized Paper 7 was very slow compared to the other paper grades. The inset (smaller figure) in *Fig7* shows that there were only small differences in absorption rate between Paper 4, 5 and 6.

Internal sizing in general is used to reduce liquid absorption into paper media and the rate at which liquid absorption occurs by adding hydrophobic substances in the paper making process. The data presented in *Figs 5* and *6* show that internal sizing (Paper 2 and 7) effectively reduces the rate at which the penetration of the water based inkjet ink droplets takes place.

Surface sizing is used to control surface porosity, enhance the internal strength of the paper media, and to provide resistance to liquid absorption. Papers 1, 2, 6 and 7 differ in that Paper 1 and 2 were not surface sized as opposed to Paper 6 and 7. The measured time for absorption into Paper 1 and Paper 6 is relatively low for both papers. In the case of Paper 2 and Paper 7, the measured time for absorption into the surface sized paper (Paper 7) is higher, which indicates that the surface sizing of this paper grade provides resistance to liquid absorption. Paper 2 and Paper 7 differ however in content and in the way they were produced which complicates an analysis of the effect of surface sizing only.

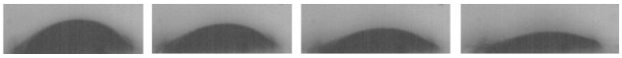

Fig 5. Absorption of an inkjet droplet on a paper surface at time= 0, 50, 100, 150 milliseconds.

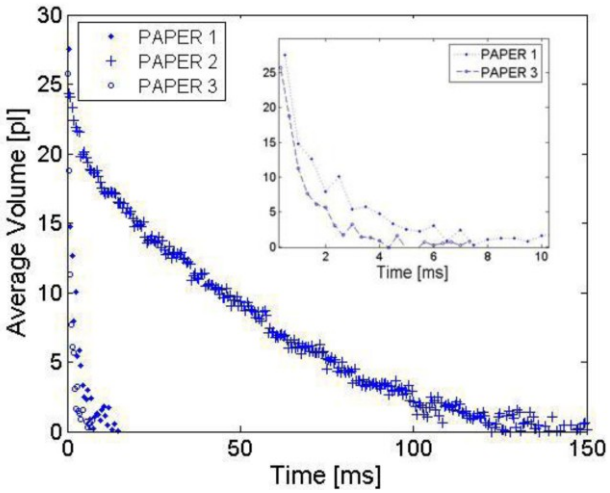

Fig 6. Average inkjet droplet volume above the paper surface as a function of time on Paper 1, 2 and 3.

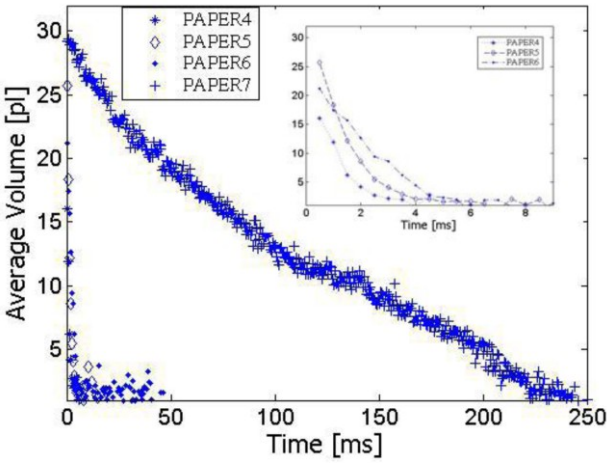

Fig 7. Average inkjet droplet volume above the paper surface as a function of time on Paper 4, 5 6 and 7.

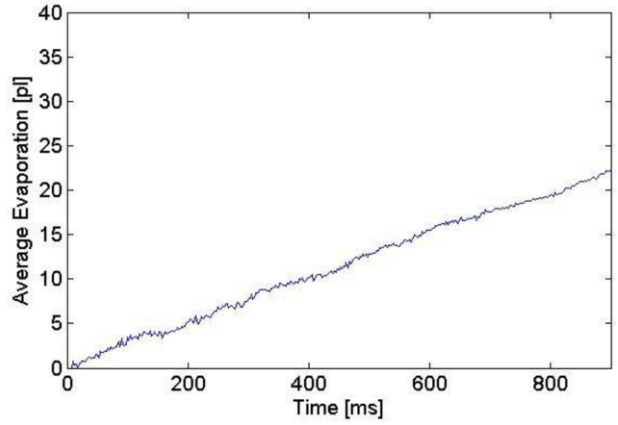

Fig 8. Average evaporated volume of an inkjet droplet on a non- porous substrate.

During the absorption process, the ink evaporates, which to some extent affects the amount of ink that absorbs into the paper. To see the effect of evaporation, film sequences of an inkjet droplet on a non-absorbing, plastic film were recorded. The evaporation is depicted in *Fig 8.*

A linear correlation between time and evaporation was observed. A least square method was therefore used to fit a linear function to data. The following relationship was found:

$$V_{evap}(t) = 23.4 \cdot t + 0.07 \qquad [9]$$

where V_{evap} is given in picolitre and time in seconds. The results from the evaporation study show that evaporation plays a role for Papers 2 and 7. Corrections for evaporation were therefore made.

Based upon the assumption of the distribution of the ink below the surface estimated from the cross-section images, the experimental penetration depth was calculated as a function of time (*Eq 4* and *5*). For Paper 4, 5 and 7 the experimental penetration depth was calculated based on the assumption that the volume has a form of a cylinder, whereas for Paper 1, 2, 3 and 6 the experimental penetration depth was calculated based on the assumption that the volume has a form of a paraboloid. In order to evaluate the time dependency of the penetration in relation to the Lucas-Washburn equation, the penetration depth was fitted to *Eq 10*.

$$d(t) = k \cdot t^a \qquad [10]$$

The constants a and k were fitted to experimental data by using a least square method.

The time dependency of the penetration is illustrated for Paper 1, 2, and 7 in *Figs 9-11*, where the solid curve represents the penetration depth according to eq. 10, with a and k given in *Table 3*, and the data points represent the experimental penetration depth (eq. 4 and 5). The penetration of inkjet ink in all of the Papers 1, 3-6 occured in roughly the same time interval. Out of these papers data for Paper 1 is shown, only (*Fig 9*).

The fitting parameters a and k for Paper 1-7 are presented in *Table 3*. The fitting parameter k (eq. 10) is lower for the internally sized papers, (Paper 2 and 7) compared to the unsized papers, (Paper 1, 3 and 6). The constant k was similar for the two coated papers (Paper 4 and 5).

A comparison between the fitting parameters a and k and the Lucas-Washburn equation was made, where the pore size peak from the Hg-porosimetry measurements was used in the Lucas-Washburn description (eq. 7). The result is presented in *Table 3*. For most paper grades, the fitting parameter a is fairly close to the time dependency of liquid penetration given by the Lucas-Washburn equation (a = 0.5). In this context it should be noted that a diffusion governed process would show the same time dependency. For all samples in table 3, however, k_{LW}, given by the Lucas-Washburn expression, is greater than the constant k, fitted to experimental data. The pore radius in the Lucas-Washburn expression was taken from *Table 2*. Defining instead the pore radius as the pore size at 50% of the cumulative volume in a Hg-porosimetry diagram showing cumulative volume versus pore size, results in the case of the uncoated papers in pore sizes of 1.2 µm to 1.4 µm (Papers 1, 2, 3 and 7) and 1.6 µm (Paper 6). This would lead to a slightly larger value of k_{LW}, but would not explain the discrepancy between the values for k_{LW} and k.

Comparing the experimental penetration depth retrieved from analysis of the video sequences in *Figs 9-11* and the cross section micrographs in *Fig 3*, the ink penetration seems to be smaller in the former case. However, the later stages of the absorption process could not be recorded with the high speed camera set-up. *Figs 9-11* indicate that the absorption process continues also after the time intervals that are presented here. In the case of the

coated papers (Papers 4 and 5), the colorant of the ink penetrates roughly 10 µm or less into the upper coating layer according to the cross section images in *Fig 3*. During absorption, parts of the ink may penetrate through the upper coating layer and reach layers having quite different properties, affecting the subsequent liquid flow. The initial absorption should however be dependent on the interaction between the ink and the upper coating layer. Moreover, the volume below the surface does not contain ink only, but consists of both paper media and ink. This should result in a larger penetration depth than accounted for here. By using the data for the void volume and the thickness of the paper samples, a correction factor was calculated for the penetration depth. The penetration depth, d, the corrected experimental penetration depth, d_{corr}, and d_{LW}, can be found in *Table 3*. The latter was estimated from eq. 7 at the time when the inkjet droplet had vanished. The corrected experimental penetration depth, d_{corr}, is in relatively good agreement with the cross section micrographs in *Fig 3* for the uncoated papers (Papers 1, 2, 3, 6 and 7). It should be noted that usage of a correction factor may not be applicable in the case of the coated papers, since these papers consist of several layers with large variations in properties.

The penetration depth, d_{LW}, described by the Lucas-Washburn equation, was found to be larger than the experimental penetration depth d. This is equivalent to k_{LW} being larger than k in *Table 2*. d_{LW} is furthermore larger than d_{corr}. Obviously, when making the assumptions described here, the Lucas-Washburn equation predicts a higher penetration depth than measured experimentally. Corrections for the ratio between void and paper do not explain this difference.

Washburn equation. In the paper media, the pores form a tortuous, interconnected void network structure, where the voids vary in size and shape. Here, the complex void network structure was described by capillaries of a representative size, retrieved from Hg porosimetry data.

Table 3. Linear fitting of data.

No	a	k $\left[\frac{mm}{s^{0.5}}\right]$	k_{LW} $\left[\frac{mm}{s^{0.5}}\right]$	d $[mm]$	Corr. fac-tor	d_{corr} $[mm]$	d_{LW} $[mm]$
1	0.44	0.143	2.22	0.015	3.54	0.053	0.17
2	0.42	0.032	0.64	0.013	3.00	0.039	0.22
3	0.51	0.239	2.23	0.012	3.74	0.046	0.12
4	0.39	0.075	0.46	0.008	7.80	0.061	0.04
5	0.44	0.072	0.40	0.006	13.6	0.087	0.03
6	0.31	0.056	5.15	0.010	3.47	0.035	0.33
7	0.57	0.016	1.30	0.007	3.45	0.023	0.58

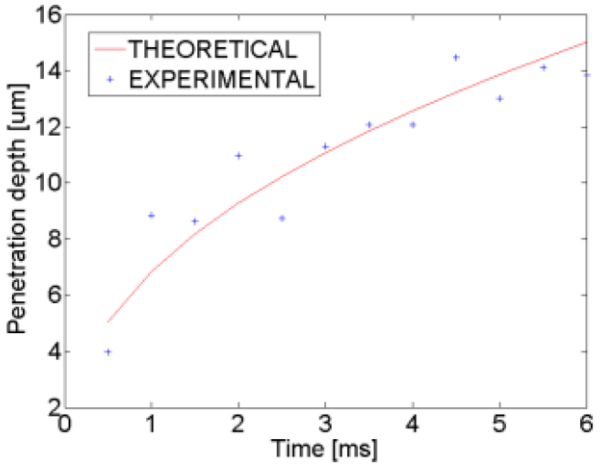

Fig 9. Linear fitting to experimental data for Paper 1.

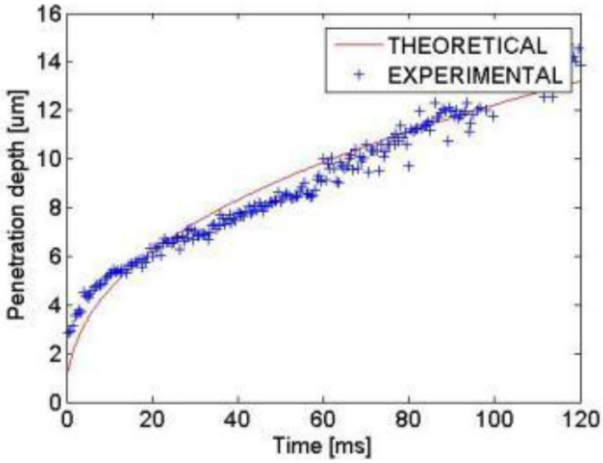

Fig 10. Linear fitting to experimental data for Paper 2.

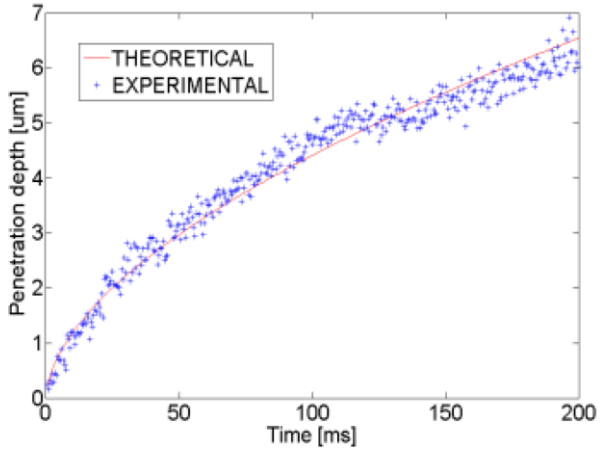

Fig 11. Linear fitting to experimental data for Paper 7.

The diameter of the inkjet ink droplets in air was roughly 40 µm, whereas pore sizes of up to roughly one or a few µm was recorded by Hg-porosimetry for the various papers. The response from Hg-porosimetry in this interval may have its origin in surface pores, pores in the base paper, or may represent the actual pore size in the paper, depending on the paper grade. The width of the

fibers at the surface of the uncoated papers is a few tens of μm and is of the same length scale as the inkjet ink droplet. Fluid transportation in the paper may take place by diffusion along the fibers or diffusion through the fibers as the fibers swell. Upon utilizing the Lucas-Washburn equation, it is assumed, however, that capillary action is the dominating transportation mechanism, and that there is a comparatively large reservoir of fluid penetrating the network. For droplets of the same length scale as the pores in the network, the latter assumption is not valid, and the liquid accessible to the capillaries may affect penetration (Danino, Marmur 1994). The flow of water based ink into the paper may also give rise to breaking of hydrogen bonds and swelling of fibers and may cause irresverible changes in the porous network, changes which are not accounted for by the Lucas-Washburn equation. It has furthermore been discussed that the Lucas-Washburn description may be inadequate due to inertial flow at intersections connecting voids of varying size (Sorbie et al. 1995, Schoelkopf et al. 2002). Moreover, the measured set of parameters is an estimation of the properties of the porous media at a microscopic level. For example, the macroscopic contact angle of a large droplet deposited on the paper surface is used to describe the dynamic contact angle of the moving meniscus inside the porous media.

This work sums up mechanisms that affect the flow of ink into paper, but does not separate the mechanisms. It can be seen in this study that the liquid penetration into papers with similar porosity varies. This might be explained by differences in the internal tortuous network structure of the papers as well as differences in the contents of the papers.

Conclusions

Absorption measurements were conducted on three pilot papers, two commercial coated inkjet papers and two commercial office papers by studies of water based dye inkjet ink droplet spreading and absorption. Internal sizing in the uncoated papers lowered the apparent surface energy, the droplet spreading and the rate of ink absorption. Evaporation played an important role in the absorption process in the case of internally sized, uncoated papers. The coated inkjet papers exhibited relatively low surface roughness and small pore sizes and gave rise to rapid inkjet ink absorption and a cylindrical distribution of the colorant of the ink in the coating layer. The penetration depth of the liquid ink in the paper media, $d(t)$, was described according to $d(t)=k \cdot t^a$ and fitted to experimental data. It was found that the time-dependency of the penetration was in accordance with the Lucas-Washburn equation, whereas the Lucas-Washburn equation overestimates the penetration depth and the speed at which the pores are filled. The assumptions made when utilizing the Lucas-Washburn equation were discussed, as well as explanations to discrepancies between the experimental results and the Lucas-Washburn equation.

Acknowledgements

The study is part of NextJet – Next Generation Substrates for Inkjet Printing (project number 2007-02402) funded by VINNOVA (The Swedish Governmental Agency for Innovation Systems), grant P32000-1, and the Kempe Foundations. The authors would also like to thank Jakob Norstedt-Moberg at Fotoverkstan and DPC for his practical support during measurements, Birgitta Sjögren, Ingrid Edin, Gunilla Eriksson and Birgitta Lundgren at MoRe research for their practical help during measurements and the cooperating companies: M-real, Kodak, and MoRe Research.

Literature

Alleborn N., Raszillier H. (2004): Spreading and sorption of droplets on layered porous substrates, J. Colloid Interface Sci, Vol 280 (2), pp 449-464

Alleborn N. and Raszillier H. (2007): Dynamics of films and droplets spreading on porous substrates, Tappi J. Vol 6 (3), pp 16-23

von Bahr, M., Tiberg, F., and Zhmud, B., (2003): Oscillations of sessile drops of surfactant solutions on solid substrates with differing hydrophobicity, Langmuir, Vol. 19 (24), pp. 10109-10115

Blake T.D., Clarke A, De Coninck J, and De Ruijter M.J., (1997): Contact angle relaxation during the spreading of partially wetting drops, Langmuir, Vol 13 (26), pp. 7293-7298

Bosanquet, C.H. (1923): On the flow of liquids into capillary tubes, Phil. Mag. Ser 6 45, 525-531

Clarke, A., Blake. T D., Carruthers. K., and Woodward. A. (2002): Spreading and Imbibition of liquid Droplets on Porous Surfaces, Langmuir, Vol 18 (8), pp 2980-2984

Daniel, R.C. and Berg J.C. (2006): Spreading on and penetration into thin, permeable print media: Application to ink-jet printing, Adv. Colloid Interface Sci., Vol 123, pp 439-469

Danino, D. and Marmur, A, (1994): Radial Capillary Penetration into paper,-Limited and unlimited liquid reservoirs, J. Colloid Interface Sci., Vol. 166 (1), pp. 245-250

Davis, S.H., and Hocking, L.M. (1999): Spreading and imbibitions of viscous liquid on a porous base, Physics of fluids, Vol. 11, pp. 48-57

Davis, S.H. and Hocking. L.M. (2000): Spreading and imbibition of viscous liquid on a porous base II, Physics of fluids, Vol. 12 (7), pp. 1646-1655

Denesuk, M., Zelinski, B.J.J., Kreidi, N.J., and Uhlman, D.R. (1994): Dynamics of incomplete wetting on porous materials, J Colloid Interface Sci, Vol 168 (1), pp. 142-151

Desie, G. and Van Roost, C. (2006): Validation of ink Media Interaction Mechanisms for Dye and pigment-based Aqeous and solvent Inks, J. Imaging Sci. Technol., Vol. 50 (3), pp. 294-303.

Fisher, L. and Lark, P.D. (1979): An experimental study of the Washburn equation for liquid flow in very fine capillaries, J. Colloid Interface Sci., Vol. 69 (3), pp. 486-492

Heilmann, J. and Lindqvist, U. (2000): Effect of drop size on the print quality in continuous ink jet printing, J. Imaging Sci. Technol., Vol 44 (6), pp. 491-494.

Heilmann, J. and Lindqvist, U. (2000): Significance of paper properties on print quality in continuous ink jet printing, J. Imaging Sci. Technol., Vol 44 (6), p. 495-499

Holman, R.K., Cima, M.J., Uhland, S.A., and Sachs E., (2002): Spreading and infiltration of inkjet-printed polymer solution droplets on a porous substrate, J. Colloid Interface Sci, Vol. 249 (2), pp 432-440

Joos, P., Van Remoortere, P., and Bracke, M. (1990): The kinetics of wetting in a capillary, J. Colloid Interface Sci. 1990, Vol. 136 (1), pp. 189-197.

Lavi, B., Marmur, A., and Bachmann, J. (2008): Porous Media Characterization by the Two-Liquid Method: Effect of dynamic Contact angle and inertia, Langmuir, Vol. 24 (5), pp. 1918-1923

Lee, K.S., Ivanova, N., Starov, V.M., Hilal, N., and Dutschk, V. (2008): Kinetics of wetting and spreading by aqueous surfactant solutions, Adv. Colloid Interface Sci., Vol 144 (1-2), pp.54–65

Lucas, R. (1918): Uber das Zeitgesetz des Kapillaren Aufstiegs von Flussigkeiten, Kolloid Z. Vol 23, pp 15-22

Lundberg, A., Örtegren, J., and Alfthan, E. (2009): On The Effect of Variations in Paper Composition On Print Quality, Conf. Proc. Non-Impact Printing 25, pp 316-319.

Martic, G., Gentner, F., Seveno, D., Coulon, D., De Coninck, J., and Blake, T.D. (2002): A molecular dynamics simulation of capillary imbibition, Langmuir, Vol. 18 (21), p. 7971-7976

Modaressi, H. and Garnier, G. (2002): Mechanism of wetting and absorption or water droplets on sized paper: Effects of chemical and physical heterogeneity, Langmuir, Vol 18 (3), pp 642-649

Ridgway, C.J., Gane, P.A.C., and Schoelkopf, J. (2002): Effect of capillary Element Aspect Ratio on the Dynamic Imbibition within Porous Networks, J. Colloid interface Sci., Vol 252 (2), pp. 373-382

Salminen, P. (1988): Studies of water transport in paper during short contact times, PhD-Thesis, Åbo Akademi University.

Schoelkopf, J., Gane, P.A.C., Ridgway, C.J., and Matthews G.P., (2000): Influence of inertia on liquid absorption into paper coating structures, Nordic Pulp Paper Res. J., Vol 15 (5), pp 422-430

Schoelkopf, J., Ridgway, C.J., Gane, P.A.C., Matthews, P., and Spielmann, D.C. (2000): Measurement and Network modeling of liquid Permeation into Compacted Mineral Blocks, J. Colloid Interface Sci., Vol. 227 (1), pp. 119-131.

Schoelkopf, J., Gane, P.A.C., Ridgway, C.J., and Matthews G.P. (2002): Practical observation of deviation from Lucas-Washburn scaling in porous media, Colloids Surf. A, Vol. 206 (1-3), 445-454

Siebold, A., Nardin, M., Schultz, J., Walliser, A., and Oppliger, M. (2000): Effect of dynamic contact angle on capillary rise phenomena, Colloids Surf., A, Vol. 161 (1), p. 81-87

Sorbie, K.S., Wu, Y.Z., and McDougall, S.R. (1995): The extended Washburn equation and its application to the oil/water pore doublet problem J. Colloid Interface Sci., Vol. 174 (2), pp 289-301.

Starov, V.M., Kosvintsev, S.R, Sobolev, V.D., Velarde, M.G., and Zhdanov, S.A. (2002): Spreading of liquid drops over saturated porous layers, J. Colloid Interface Sci,, Vol 246 (2), pp. 372-379

TAPPI T 558 om-97: Surface wettability and absorbency of sheeted materials using an automated contact angle tester

Washburn, E.W. (1921): The Dynamics of capillary flow, Phys.Rev., Vol 17, pp. 273-283.